

This discussion paper is/has been under review for the journal Earth Surface Dynamics (ESurfD).
Please refer to the corresponding final paper in ESurf if available.

Analyzing bed and width oscillations in a self-maintained gravel-cobble bedded river using geomorphic covariance structures

R. A. Brown^{1,2} and G. B. Pasternack¹

¹University of California, Davis, One Shields Avenue, Davis, CA, USA

²Environmental Science Associates, 2600 Capitol Avenue, Suite 200, Sacramento, CA, USA

Received: 5 December 2015 – Accepted: 10 December 2015 – Published: 5 February 2016

Correspondence to: R. A. Brown (rokbrown@ucdavis.edu)

Published by Copernicus Publications on behalf of the European Geosciences Union.

ESURFD

doi:10.5194/esurf-2015-49

Analyzing river bed and width oscillations

R. A. Brown and
G. B. Pasternack

Title Page

Abstract

Introduction

Conclusions

References

Tables

Figures



Back

Close

Full Screen / Esc

Printer-friendly Version

Interactive Discussion



Abstract

This paper demonstrates a relatively new method of analysis for stage dependent patterns in meter-scale resolution river DEMs, termed geomorphic covariance structures (GCSs). A GCS is a univariate and/or bivariate spatial relationship amongst or between variables along a pathway in a river corridor. Variables assessed can be flow independent measures of topography (e.g., bed elevation, centerline curvature, and cross section asymmetry) and sediment size as well as flow dependent hydraulics (e.g., top width, depth, velocity, and shear stress; Brown, 2014), topographic change, and biotic variables (e.g., biomass and habitat utilization). The GCS analysis is used to understand if and how the covariance of bed elevation and flow-dependent channel top width are organized in a partially confined, incising gravel-cobbled bed river with multiple spatial scales of anthropogenic and natural landform heterogeneity across a range of discharges through a suite of spatial series analyses on 6.4 km of the lower Yuba River in California, USA. A key conclusion is that the test river exhibited positively covarying and quasi-periodic oscillations of bed elevation and channel width that had a unique response to discharge as supported by several tests. As discharge increased, the amount of positively covarying values of bed elevation and flow-dependent channel top width increased up until the 1.5 and 2.5 year annual recurrence flow and then decreased at the 5 year flow before stabilizing for higher flows. These covarying oscillations are quasi-periodic scaling with the length scales of pools, bars, and valley oscillations. Thus, it is the ~~fact~~ that partially confined gravel-cobble bedded alluvial rivers organize their adjustable topography with a preference for covarying and quasi-periodic bed and width undulations at channel forming flows due to both local bar-pool mechanisms and non alluvial topographic controls.

ESURFD

doi:10.5194/esurf-2015-49

Analyzing river bed and width oscillations

R. A. Brown and
G. B. Pasternack

Title Page

Abstract

Introduction

Conclusions

References

Tables

Figures



Back

Close

Full Screen / Esc

Printer-friendly Version

Interactive Discussion



1 Introduction

Understanding the spatial organization of river systems in light of natural and anthropogenic change is extremely important, because we can provide information to assess, manage and restore them to ameliorate worldwide freshwater fauna declines (Richter et al., 1997). Alluvial rivers found in transitional upland-lowland environments with slopes ranging from 0.005 to 0.02 and median diameter bed sediments ranging from 8 to 256 mm can exhibit scale dependent organization of their bed sediments (Milne, 1982), bed elevation profile (Madej, 2001), cross section geometry (Rayberg and Neave, 2008) and morphological units (Wyrick and Pasternack, 2014). For these types of river channels a plethora of studies spanning analytical, empirical and numerical domains suggest that at channel forming flows there is a preference for positively covarying bankfull bed and width undulations amongst morphologic units such as pools and riffles. That is, relatively wide areas have higher relative bed elevations and the converse. While covarying bed and width undulations have been evaluated in field studies using cross section data (Richards, 1976a, b), in models of sediment transport and water flow (Repetto and Tubino, 2001), and in theoretical treatments (Huang et al., 2004), this idea has never been evaluated in a self-maintained bankfull river channel for which a meter-scale digital elevation model is available across a wide range of discharges from a fraction of to orders of magnitude more than bankfull. The focus of this paper is twofold. First, we aim to demonstrate how meter-scale resolution topography can be analyzed with hydraulic model outputs to generate flow dependent geomorphic covariance structures of bed elevation and wetted width. A GCS is a univariate and/or bivariate spatial relationship amongst or between variables along a pathway in a river corridor. Variables assessed can be flow independent measures of topography (e.g., bed elevation, centerline curvature, and cross section asymmetry) and sediment size, as well as flow dependent hydraulics (e.g., top width, depth, velocity, and shear stress; Brown, 2014), topographic change, and biotic variables (e.g., biomass and habitat utilization). Second, we aim to use these methods and concepts to understand if and how

ESURFD

doi:10.5194/esurf-2015-49

Analyzing river bed and width oscillations

R. A. Brown and
G. B. Pasternack

Title Page

Abstract

Introduction

Conclusions

References

Tables

Figures



Back

Close

Full Screen / Esc

Printer-friendly Version

Interactive Discussion



bed elevation and flow-dependent channel width are organized in a partially confined, incising gravel-cobbled bed river with multiple spatial scales of landform heterogeneity across a range of discharges through a suite of spatial series analyses on 9 km of the lower Yuba River (LYR) in California, USA.

1.1 Background

A multitude of numerical, field, and theoretical studies have shown that gravel bed rivers have covarying oscillations between bed elevation and channel width related to riffle-pool maintenance. The joint periodicity in oscillating thalweg and bankfull width series for pool-riffle sequences in gravel bed rivers was first identified by Richards (1976b) who noted that riffles have widths that are greater on average than pools, and he attributed this to flow deflection over riffles into the channel banks. Since then, many studies related to bar and pool maintenance have implied a specific spatial covariance of width and depth between the pool and riffle at the bankfull or channel forming discharge (Wilkinson et al., 2004; MacWilliams et al., 2006; Caamano et al., 2009; Thompson, 2010). For example, Caamano et al. (2009) derived a criterion for the occurrence of a mean reversal in velocity (Keller, 1971) that implies a specific covariance of the channel geometry of alluvial channels with undulating bed profiles. For a reversal in mean velocity at the bankfull or channel forming discharge the riffle must be wider than the pool and the width variation should be greater than the depth variation between the riffle and residual pool depth. Milan et al. (2001) evaluated several riffle pool couplets, from a base flow to just over the bankfull discharge. They found that convergence and reversals in section-averaged velocity and shear stress were complex and non-uniform, which suggests that different morphologic units may be maintained at different discharges. Wilkinson et al. (2004) explicitly showed that phase shifts in shear stress from the riffle to the pool between high and low discharge required positively covarying bed and width undulations. White et al. (2010) showed how valley width oscillations influence riffle persistence despite larger channel altering floods and inter-decadal valley incision. Sawyer et al. (2010) used two-dimensional (2-D) hydrodynamic

Analyzing river bed and width oscillations

R. A. Brown and
G. B. Pasternack

Title Page

Abstract

Introduction

Conclusions

References

Tables

Figures



Back

Close

Full Screen / Esc

Printer-friendly Version

Interactive Discussion



modeling and digital elevation model (DEM) differencing to illustrate how variations in wetted width and bed elevation can modulate regions of peak velocity and channel change at a pool-riffle-run sequence across a range of discharges from 0.15 to 7.6 times bankfull discharge. DeAlmeida and Rodriquez (2012) used a morphodynamic model to recreate riffle-pool bedforms after removing the initial bed profile and using the width profile, showing that channel width can exert controls on the structure of the bed profile.

From a system perspective bed and width undulations, both jointly and in isolation, have been suggested to be a means of self-adjustment in alluvial channels that minimize the time rate of potential energy expenditure per unit mass of water in accordance with the law of least time rate of energy expenditure (Langbein and Leopold, 1962; Yang, 1971; Cherkauer, 1973; Wohl et al., 1999). For bed profiles, Yang (1971) and Cherkauer (1973) showed that undulating bed relief is a preferred configuration of alluvial channels that minimize the time rate of potential energy expenditure. Using field, flume, and numerical methods Wohl et al. (1999) showed that valley wall oscillations also act to regulate flow energy analogous to bedforms. In analyzing reach scale energy constraints on river behavior Huang et al. (2004) quantitatively showed that wide and shallow and deep and narrow channels are two end member cross sectional configurations necessary for efficiently expending excess energy for rivers, so these two types of cross sections imply covarying bed and width undulations as a means of expending excess energy. Therefore the above studies suggest that both bed and width oscillations are a means to optimize channel geometry for the dissipation of excess flow energy.

Many of the studies discussed above have shown the presence and geomorphic role of positively covarying bed and width undulations for a limited range of discharges, rarely above bankfull discharge. However, many rivers exhibit multiple scales of freely formed and forced landscape heterogeneity that should influence fluvial geomorphology when the flow interacts with them (Church, 2006; Gangodagamage et al., 2007). Given that positive bed and width undulations can control channel maintenance at

ESURFD

doi:10.5194/esurf-2015-49

Analyzing river bed and width oscillations

R. A. Brown and
G. B. Pasternack

Title Page

Abstract

Introduction

Conclusions

References

Tables

Figures

⏪

⏩

◀

▶

Back

Close

Full Screen / Esc

Printer-friendly Version

Interactive Discussion



and near bankfull discharge, it is hypothesized that it could also do so at other discharges, as other topographic features are activated with increasing discharge (Brown and Pasternack, 2014). However, in river corridors a more complete understanding of form, and ultimately process, can be gleaned from considering how landforms steer water at different flows (Brown and Pasternack, 2014). Traditional geomorphometry relies on analyzing landform topography in the absence of water flow (Pike et al., 2008). The coupling of meter-scale topography with commensurate hydraulic models (see the Supplement) is thought of as an advancement to geomorphometry. Given the increasing abundance of remotely sensed data for alluvial rivers, and the ability to model large segments of entire river corridors, this could be an important tool for land managers to understand the topographic structure of river corridors.

1.2 Study objectives

This study sought to evaluate the longitudinal geomorphic covariance structure of bed and width undulations in a river valley for a wide range of discharges above and below the bankfull discharge ~~never evaluated before~~. The primary goal of this study was to determine if there are covarying bed and width oscillations in an incising gravel/cobble river, if they exhibit any periodicity, and whether they vary with discharge. A secondary objective is to demonstrate how geomorphic covariance structures for bed and width can be generated from high-resolution topography and hydraulic models. The study site was a 6.4 km section of the lower Yuba River (LYR), an incising and partially confined self-formed gravel-cobble bedded river (Fig. 1; described in Sect. 3). Several statistical tests were used on the serial covariance of bed elevation, Z , channel top width, W^j , and their covariance, $C(Z, W^j)$, where j notes the flow discharge. The novelty of this study is that it provides the first assessment of flow-dependent bed and width covariance in a partially confined, self-maintained alluvial river across a wide array of flows. The broader impact is that it provides a framework for analyzing the flow dependent topographic variability of river corridors, without differentiating between discrete landforms such as riffles and pools. Further, an understanding of the flow dependent

Analyzing river bed and width oscillations

R. A. Brown and
G. B. Pasternack

Title Page

Abstract

Introduction

Conclusions

References

Tables

Figures



Back

Close

Full Screen / Esc

Printer-friendly Version

Interactive Discussion



spatial structure of bed and width GCS would be useful in assessing their utility in applied river corridor analysis and synthesis for river engineering, management and restoration.

2 Experimental design

5 To evaluate covarying bed and width undulations the concepts and methods of geomorphic covariance structures (GCSs) were used (Brown, 2014; Brown and Pasternack, 2014). GCSs are univariate and/or bivariate spatial relationships amongst or between variables along a pathway in a river corridor. Variables assessed can be flow independent measures of topography (e.g., bed elevation, centerline curvature, and cross section asymmetry) and sediment size as well as flow dependent hydraulics (e.g., top
10 width, depth, velocity, and shear stress; Brown, 2014), topographic change, and biotic variables (e.g., biomass and habitat utilization). Calculation of a GCS from paired series is relatively straightforward by the cross product $x_{\text{std},i} \times y_{\text{std},i}$, where the subscript std refers to standardized and detrended values of two variables x and y at location i
15 along the centerline, creating the serial data set of covariance, $C(XY)$. Since this study is concerned with bed and flow dependent top width undulations, the GCS at each flow j is denoted as $C(Z, W^j)$. More information on GCS theory is provided in Sect. 4.2 below.

20 GCS series were generated for eight flows ranging from 8.50 to 3126 m³ s⁻¹, spanning a broad range of flow frequency (Table 1). The first question this study sought to answer was if there was a preference for $C(Z, W^j)$ to positively covary and how it changed with discharge. To analyze this a histogram was generated for each flow dependent series of $C(Z, W^j)$ that was stratified by the signs of bed elevation, Z , and wetted width, W^j , to see if there was a preference for positive $C(Z, W^j)$. The second
25 question was whether $C(Z, W^j)$ was random or quasi-periodic. To answer this question autocorrelation function (ACF) and power spectral density (PSD) analyses of each

Analyzing river bed and width oscillations

R. A. Brown and
G. B. Pasternack

Title Page

Abstract

Introduction

Conclusions

References

Tables

Figures



Back

Close

Full Screen / Esc

Printer-friendly Version

Interactive Discussion



$C(Z, W^j)$ series were used to determine if there were quasi-periodic length scales that $C(Z, W^j)$ covary and how that changes with discharge.

Based on the studies listed above (Sect. 1.1), we hypothesize that there should be a preference for positively covarying residuals of $C(Z, W^j)$ for discharges with annual recurrence intervals from 1.25–5 years (Williams, 1978; Andrews, 1980; Nolan et al., 1987), but other complex responses are possible. The basis for positive $C(Z, W^j)$ is founded on the idea that, on average, channel geometry is maintained during bankfull (e.g. geometric bankfull) discharge (Williams, 1978) and that locally channels are shaped by riffle-pool maintenance mechanisms (Wilkinson et al., 2004; MacWilliams et al., 2006; Caamano et al., 2009; Thompson, 2010). Thus, with changes in flow we hypothesize that the residuals of the $C(Z, W^j)$ GCS will, on average, become more positive with increasing flow until the bankfull discharge, where the channel overtops its banks and non-alluvial floodplain features exert control on cross-sectional mean hydraulics. At that point there may not be a preference for positive or negative residuals. With this logic, it's hypothesized that the $C(Z, W^j)$ GCS will be quasi-periodic for flows at and below the bankfull discharge, due to the presence of bar and pool topography, and that the ACF and PSD will yield length scales commensurate with the average spacing of these topographic features. For flows above the bankfull discharge it is unknown how length scales will change, necessitating this study. In addition to performing these tests we also present two ~ 1.4 km sections of the $C(Z, W^j)$ GCS, Z , W and the detrended topography for three representative flows to discuss specific examples of how these patterns change with landforms in the river corridor across a wide array of discharges.

Limitations to this study (but not the GCS approach) for worldwide generalization include not considering other variables relevant to how alluvial rivers adjust their shape such as grain size, channel curvature and vegetation, to name a few. Some of these limitations were not study oversights, but reflected the reality that the study reach used had relatively homogenous sediments (Jackson et al., 2013), low sinuosity, and limited vegetation (Abu-Aly et al., 2014). This yielded an ideal setting to determine how much

Analyzing river bed and width oscillations

R. A. Brown and
G. B. Pasternack

Title Page

Abstract

Introduction

Conclusions

References

Tables

Figures

◀

▶

◀

▶

Back

Close

Full Screen / Esc

Printer-friendly Version

Interactive Discussion



Discussion Paper | Discussion Paper | Discussion Paper | Discussion Paper | Discussion Paper | Discussion Paper | Discussion Paper | Discussion Paper | Discussion Paper

order was present for ~~just~~ bed elevation and channel width, but does not disregard the importance of these other controls, which can be addressed in future studies at suitable sites.

3 Study area

The study site was the 6.4 km reach of the ~~Timbuctoo Bend located on the~~ Lower Yuba River (LYR) in California, USA. (The LYR is an incising and partially confined gravel-cobble bedded river with a mixture of alluvial channel patterns ranging from weakly anabranching to meandering. For the study area the average slope, bankfull width to depth ratio ~~at bankfull~~, sinuosity, and mean grain size were 2%, 82, 1.1, and 164 mm, respectively (Wyrick and Pasternack, 2012). Vegetated cover of the river corridor ranged from 0.8–8.1% of the total wetted area at each flow, with more inundated vegetation at higher flows. The flows analyzed in this study ranged from 8.50 to 3126 m³ s⁻¹, and their recurrence intervals are shown in Table 1. Wyrick and Pasternack (2012) analyzed inundation patterns in the river corridor as channel and floodplain shapes change dramatically through the study reach. Different locations exhibit spillage out of the channel into low-lying peripheral swales and onto lateral and point bars at flows from ~ 28.32–141.6 m³ s⁻¹. When the water stage rises to 141.6 m³ s⁻¹, relatively flat active bar tops become inundated and it lines up with the base of willows along steeper banks flanking the channel where it is well defined. These and other field indicators led to the consideration of 141.6 m³ s⁻¹ as representative of the bankfull discharge adjusted to the modern regulated flow regime since 1970. By a flow of 198.2 m³ s⁻¹, banks are all submerged and water is spilling out to various degrees onto the floodplain. The floodplain is considered inundated when the discharge reaches 597.5 m³ s⁻¹. Above that flow stage ~~exist~~ some terraces, bedrock outcrops, and soil-mantled hillsides ~~that~~ become inundated. In two locations there are wide relict dredger tailings piles on the inside of the two uppermost meander bends that the river has been gradually eroding and that interact with the flows ranging from 597.5–1195 m³ s⁻¹.

Analyzing river bed and width oscillations

R. A. Brown and
G. B. Pasternack

Title Page

Abstract

Introduction

Conclusions

References

Tables

Figures

◀

▶

◀

▶

Back

Close

Full Screen / Esc

Printer-friendly Version

Interactive Discussion



Apart from these piles, the flow width interacts predominately with the valley walls for discharges at $1195 \text{ m}^3 \text{ s}^{-1}$ and above.

Historically the LYR was impacted by hydraulic gold mining in the late 1800's and dam construction in the mid 1900's. Mining sediments initially overwhelmed the river corridor (James, 2009), but dam construction to retain sediment blocked further upstream input and lessened this impact over time as the river gradually has incised into these deposits (Adler, 1980; Carley et al., 2010). Despite these impacts the LYR still experiences significant channel changing flood flows (Carley et al., 2010; Brown and Pasternack, 2014), as two of three sub catchments do not have large dams. Englebright Dam, located approximately 3 km upstream of the study area is kept nearly full and overtops when outflow is $> 127.4 \text{ m}^3 \text{ s}^{-1}$, so flood hydrology is still seasonal and driven by rainfall and snowmelt.

Several existing studies can help put the study section into its hydrogeomorphic context. White et al. (2010) used aerial photography and a qualitative analysis of repeat long profiles and valley width series in a valley confined reach to conclude that valley width oscillations controlled longitudinal riffle locations for several decades even as the reach incised dramatically. Sawyer et al. (2010) found that one of the riffles in this reach experienced flow convergence routing between baseflow, bankfull flow, and a flow of ~ 8 times bankfull discharge that maintained riffle relief. More recently the entire LYR was studied with $\sim 0.5\text{--}5$ m resolution for geomorphic change detection (Carley et al., 2010), morphological unit mapping (Wyrick and Pasternack, 2012, 2014), and the role of spatially distributed vegetative roughness on flood hydraulics, as simulated using a two-dimensional (2-D) hydrodynamic model (Abu-Aly et al., 2013). This study builds on these in several ways. First, this study directly evaluates the relationship between bed elevation and flow width for a range of discharges, which furthers and improves upon the study by White et al. (2010) that did not assess stage dependence nor perform rigorous quantitative tests. Second, this study uses 2-D-model-derived wetted width outputs from the LYR 2-D model of Abu-Aly et al. (2013) and thus advances what one can glean from such data sets. Further, morphological unit mapping by Wyrick and

Analyzing river bed and width oscillations

R. A. Brown and
G. B. Pasternack

Title Page

Abstract

Introduction

Conclusions

References

Tables

Figures



Back

Close

Full Screen / Esc

Printer-friendly Version

Interactive Discussion



Analyzing river bed and width oscillations

R. A. Brown and
G. B. Pasternack

Title Page

Abstract

Introduction

Conclusions

References

Tables

Figures

◀

▶

◀

▶

Back

Close

Full Screen / Esc

Printer-friendly Version

Interactive Discussion



Pasternack (2012, 2014) is used to contextualize length scales (and thus frequency) associated with pool, riffle, and point bars. Not all morphological units are associated with only lateral and vertical undulations of channel topography, but pool, riffle, and point bar spacing's were thought to be useful in contextualizing length scales for the ACF and PSD analysis. Finally, this study evaluates the organization of channel geometry in light of a study that quantified the magnitude and extent of statistically significant channel change for the entire lower Yuba River (Carley et al., 2012). The overall response was dictated by knickpoint migration, bank erosion and overbank deposition processes. They found there was a decreasing trend of mean vertical incision rates, ranging from approximately -15 cm yr^{-1} at the upper limit of this study to almost none at the lower limit, showing that upstream knickpoint migration is driving channel change (e.g. Fig. 11 in Carley et al., 2010). Overall these studies show that the river corridor is still adjusting to upstream sediment regulation (Carley et al., 2010), yet sites have achieved self-maintenance of persistent topographic forms (Saywer et al., 2010; White et al., 2010) and exhibit a highly diverse assemblage of fluvial landforms (Wyrick and Pasternack, 2014).

4 Methods

To test the study hypotheses Z_i and W^j series were extracted from the meter-scale topographic map of the Lower Yuba River produced from airborne LiDAR, echosounder, and ground surveys (Carley et al., 2012; see Supplement). A meter-scale 2-D hydrodynamic model was used to generate data sets for wetted width for each discharge. Details about the 2-D model are documented in the Supplement and previous publications (Abu-Aly et al., 2013; Wyrick and Pasternack, 2014; Pasternack et al., 2014); it was thoroughly validated for velocity vector and water surface elevation metrics, yielding outcomes on par or better than other publications using 2-D models.

4.1 Data extraction

A first step was to extract minimum bed elevation and top width spatial series from the digital elevation model and 2-D model outputs. This required having a sample pathway along which bed elevation could be extracted from the DEM and top width from the wetted extents from the 2-D model. Sampling river widths was done using cross sections that are generated at even intervals perpendicular to the sample pathway and then clipped to the 2-D model derived wetted extents for each flow. Because of this, the pathway selected can have a significant bearing on whether or not sample sections represent downstream oriented flow or overlap where pathway curvature is high. There are several options in developing an appropriate pathway for sampling the river corridor. The thalweg is commonly used in flow-independent geomorphic studies, but since there are sub-channel-width forced scour holes adjacent to local bedrock outcrops, the thalweg is too tortuous within the channel to adhere to a reasonable definition of top width. Further, as flow increases, flow path deviates from the deepest part of the channel due to topographic steering from submerged and partially submerged topography (Abu-Aly et al., 2014). Therefore, in this study we manually developed flow-dependent sample pathways using 2-D model hydraulic outputs of depth, velocity and wetted area. The effect of having different sample pathways for each flow is that it accounts for flow steering by topographic features in the river corridor. Some sample pathways were similar, as inundation extents were governed by similar topographic features. Namely, 283.2 and 597.5 m³ s⁻¹ were very similar, as were 2390 and 3126 m³ s⁻¹. Since each sample pathway was flow dependent, the lengths decreased with discharge, as features that steer flow at lower discharges can be submerged at higher discharges. This is in line with theories of maximum flow efficiency in rivers (Huang et al., 2004), and broader concepts such as constructal theory for the design of natural systems (Bejan and Lorente, 2010).

For each flow a conveyance grid ($d_i \times v_i^2$) was generated in ARCGIS[®], where d_i is the depth and v_i is the velocity at node i in the 2-D model hydraulics rasters. Then

ESURFD

doi:10.5194/esurf-2015-49

Analyzing river bed and width oscillations

R. A. Brown and
G. B. Pasternack

Title Page

Abstract

Introduction

Conclusions

References

Tables

Figures

◀

▶

◀

▶

Back

Close

Full Screen / Esc

Printer-friendly Version

Interactive Discussion



Analyzing river bed and width oscillations

R. A. Brown and
G. B. Pasternack

Title Page

Abstract

Introduction

Conclusions

References

Tables

Figures



Back

Close

Full Screen / Esc

Printer-friendly Version

Interactive Discussion



a sample pathway was manually digitized using the conveyance grid, following the path of greatest conveyance. For flow splits, if the magnitude of conveyance in one channel was more than twice as great as the other it was chosen as the main pathway. If they were approximately equal then the pathway was centered between the split.

5 Once a sample pathway was developed it was then smoothed over a range of 100 m, or approximately a bankfull channel width to help further minimize section overlaps. Still there are some areas of the river where the river has relatively high curvature in the sample pathway causing sample section overlaps to occur. These were manually edited by visually comparing the sample sections with the conveyance grid and removing overlapped sections that did not follow the downstream flow of water. This was more prevalent at the lower discharges than the higher ones due to the effects topographic steering creating more variable sample pathways. After overlaps were removed, the data was linearly interpolated between the remaining sections to match the original sampling frequency. Before sections were clipped to the wetted extents, any backwater or non downstream oriented areas were removed. For bed elevation, Z , the minimum value along each section was sampled from the DEM using the same sections for measuring width for each flow. All data were sampled at intervals of 5 m ($\sim 6\%$ of the average bankfull width), giving a sampling frequency of $0.2 \text{ cycles m}^{-1}$ and cutoff frequency of $0.1 \text{ cycles m}^{-1}$.

4.2 Developing geomorphic covariance structures

To generate GCS series for bed and flow dependent width undulations the two variables, Z and W^j were first detrended and standardized. Minimum bed elevation data, Z , were detrended using a linear model (Table 2) as is common in many studies that analyze reach scale bed variations (Melton, 1962; Richards, 1976a; McKean et al., 2008). Similarly, each flow dependent width series was linearly detrended, but the trends were relatively low (Table 2). Finally, each series was standardized by the mean and variance of the entire series (Salas et al., 1980) to achieve second order stationarity, which is a prerequisite for spectral analysis. Removal of the lowest frequency of a signal, which

can often be visually assessed, has little impact upon subsequent spectral analyses (Richards, 1979). A linear trend was used over other options such as a polynomial because a linear trend preserves the most amount of information in the bed series, while a polynomial can effectively filter out potential oscillations. It is important to note that standardization by the mean and variance of each series makes each dataset dependent on the length analyzed. This has the effect that the magnitude and potentially the sign of $C(Z, W^j)$ at specific locations are not similar if different lengths of a river are analyzed. Once detrended and standardized series of Z and W^j were generated the GCS was created by taking the cross product of the two at each centerline station, yielding $C(ZW^j)$ as shown in Fig. 2. Interpretation of a GCS is based on the sign of the covariance and that of contributing terms. If both Z and W^j are positive or negative then $C(Z, W^j) > 0$, but if only one is negative then $C(Z, W^j) < 0$. For $C(Z, W^j)$ these considerations yield four sub-reach scale landform end members that deviate from normative conditions (Fig. 3). Due to the statistical transformation of the raw data to detrended and standardized values, normative conditions are those close to zero. These landforms are not the same as classic zero-crossing riffles and pools (e.g. Carling and Orr, 2000), because they explicitly account for bed and width variation. Neither are they the same as laterally explicit morphological units (Wyrick and Pasternack, 2014), because they average across the full channel width. Also, both of those types of landforms are flow independent, whereas the landforms identified herein are flow-dependent to ascertain the combined functionality of flow and topography in terms of overall flow conveyance. Note that the signs of Z and W^j are not only important, but the magnitude of the covariance is, too. Since $C(Z, W^j)$ is generated by multiplication, if either Z or W^j is < 1 or > -1 it serves to discount the other, while if Z or W^j is > 1 or < -1 it amplifies $C(Z, W^j)$. To assess the statistical significance of coherent landform patterns we utilize a similar threshold of ± 1 for statistical significance following Brown and Pasternack (2014).

ESURFD

doi:10.5194/esurf-2015-49

Analyzing river bed and width oscillations

R. A. Brown and
G. B. Pasternack

Title Page

Abstract

Introduction

Conclusions

References

Tables

Figures

◀

▶

◀

▶

Back

Close

Full Screen / Esc

Printer-friendly Version

Interactive Discussion



4.3 Data analysis

Before any statistical tests were performed we first visually assessed the data in two approximately 1.4 km long sections to illustrate how $C(Z, W^j)$ is affected by flow responses to landforms. For these two examples only three discharges were selected to illustrate flow dependent changes in Z , W^j , and $C(Z, W^j)$ with fluvial landforms. The lowest and highest flows, e.g. 8.50 and 3126 m³ s⁻¹, were selected to bracket the range of flows investigated. The intermediate flow selected was 283.2 m³ s⁻¹ based on the shifts in $C(Z, W^j)$ observed in the histogram, ACF and PSD tests as shown below in the results. For these examples the exact magnitudes of $C(Z, W^j)$ are not as important as the patterns and how they relate to visually discernible landforms. However, the term “significant” will be used when any series is > 1 or < -1 as in Brown and Pasternack (2014).

A Mann–Whitney U test was performed between each $C(Z, W^j)$ dataset to determine if they were statistically different at the 95 % level. Histograms were then computed for each $C(Z, W^j)$ dataset to evaluate whether there was a preference for the data to be positively covarying and how that changes with discharge. Two histograms were developed, one based on the quadrant classification of $C(Z, W^j)$ for each flow and another showing the magnitudes of covariance. This was done so that the distribution of both the type of covariance and magnitudes could be assessed. Additionally, the bivariate Pearson’s correlation coefficients (r) were computed between Z and W^j to assess their potential interdependence. Bivariate Pearson’s correlation coefficients were also computed for each series of W^j . Since this analysis requires series of equal length width sections for each W^j were mapped to the bankfull centerline at 141.6 m³ s⁻¹ using the near function in ARCGIS[®]. Statistical significance was assessed for (r) using a white noise null hypothesis at the 95 % level.

Next, two complimentary tests were used to determine if $C(Z, W^j)$ was quasi-periodic or random. Since the PSD is derived from the ACF the two tests show the same information, but in different domains, with the ACF in the space domain and the PSD

Analyzing river bed and width oscillations

R. A. Brown and
G. B. Pasternack

Title Page

Abstract

Introduction

Conclusions

References

Tables

Figures



Back

Close

Full Screen / Esc

Printer-friendly Version

Interactive Discussion



in the frequency domain. Both are shown to visually reinforce the results of the PSD analysis. This is helpful because spectral analysis can be very sensitive to the algorithm used and associated parameters such as window type and size. Showing the ACF allows a visual check of dominant length scales that may have quasi-periodicity.

5 The ACF analysis was performed for each flow dependent series of $C(Z, W^j)$ and then these were compared among flows to characterize stage dependent variability and to analyze how spatial structure changed with discharge. This test essentially determines the distances over which $C(Z, W^j)$ are similar. An unbiased estimate of autocorrelation for lags was used:

$$10 R_k = \frac{\frac{1}{n-k} \sum_{i=1}^{n-k} (x_i - \bar{x})(x_{i+k} - \bar{x})}{\frac{1}{n} \sum_{i=1}^{n-k} (x_i - \bar{x})^2} \quad (1)$$

where the terms $\frac{1}{n-k}$ and $\frac{1}{n}$ account for sample bias (Cox, 1983; Shumway and Stoffer, 2006). Each R_k vs. lag series was plotted against discharge for a maximum of 640 lags (3.2 km, or approximately half the study length), creating a surface that shows how ACF evolves with flow. Statistical significance was assessed relative to white and red noise autocorrelations, where the latter is essential a first order Markov process (Newland, 1993). The benefit of this approach is that (i) many fluvial geomorphic spatial series display autoregressive properties (Melton, 1962; Rendell and Alexander, 1979; Knighton, 1983; Madej, 2001) and (ii) it provides further context for interpreting results beyond assuming white noise properties. The 95 % confidence limits for white noise are given by $-\frac{1}{n} \pm \frac{2}{\sqrt{n}}$ (Salas et al., 1980). For red noise, a first order autoregressive (AR1) model was fit to the standardized residuals for each spatial series of bed elevation and channel width. For comparison, first order autoregressive (AR1) models were produced for 100 random spatial series (each with the same number of points as the flow width spatial series) and averaged. Each averaged AR1 flow width series was then multiplied

Analyzing river bed and width oscillations

R. A. Brown and
G. B. Pasternack

Title Page	
Abstract	Introduction
Conclusions	References
Tables	Figures
◀	▶
◀	▶
Back	Close
Full Screen / Esc	
Printer-friendly Version	
Interactive Discussion	



Analyzing river bed and width oscillations

R. A. Brown and
G. B. Pasternack

Title Page

Abstract

Introduction

Conclusions

References

Tables

Figures

◀

▶

◀

▶

Back

Close

Full Screen / Esc

Printer-friendly Version

Interactive Discussion



against the AR1 bed elevation series to create an AR1 model for each $C(Z, W^j)$. The red noise estimate was then taken as the average of all AR1 models of $C(Z, W^j)$. The ACF plots were made so that values not exceeding the white noise significance are not shown, along with a reference contour for the AR1 estimate. Frequencies can be gleaned from the ACF analysis by taking the inverse of the lag distance associated repeating peaks following Carling and Orr (2002).

Power spectral density was estimated for each $C(Z, W^j)$ series using a modified periodogram method as an additional test for periodicity (Carter et al., 1973). The periodogram is the Fourier transform of the biased estimate of the autocorrelation sequence. The modified periodogram is defined as:

$$P(f) = \frac{\Delta x}{N} \left| \sum_{n=0}^{N-1} h_n x_n e^{-i2\pi f n} \right|^2 \quad (2)$$

where $P(f)$ is the power spectral density of x , h_n is the window, Δx is the sample rate, and N is the number of data data points (Trauth et al., 2006). While the raw periodogram can exhibit spectral leakage, a window can reduce this effect. A hamming window was used with a length equal to each data set. Since samples were taken every 5 m, this resulted in a sampling frequency of $0.2 \text{ cycles m}^{-1}$, and a Nyquist frequency, or cutoff of $0.1 \text{ cycles m}^{-1}$. The number of data points used for the analysis was roughly half the largest data set, resulting in a bandwidth of $0.00016 \text{ cycles m}^{-1}$. For PSD estimates a modified Lomb–Scargle confidence limit for white noise at the 95 % level was used as recommended by Hernandez (1996). Since this study was concerned with changes in PSD with flow, estimates were plotted relative to the standard deviation of all PSD results for all series. This was done instead of using the standard deviation of each series, because that erroneously inflates power within a series without context for the variance of adjacent flows.

It's important to note that the sample pathway, and thus stationing, changes with each flow, due to having flow dependent sample pathways to account for topographic

positive peak in $C(Z, W^j)$, but reducing its magnitude from $283.2 \text{ m}^3 \text{ s}^{-1}$ flow. As flow fully overtops the alternate bars the sign of the oscillatory pattern of W for the alternate bar section reverses from the pattern at the $283.2 \text{ m}^3 \text{ s}^{-1}$, but $C(Z, W^j)$ is still low since Z is close to zero.

5.2 Is there a preference for positively covarying bed and width oscillations?

The histogram of $C(Z, W^j)$ showed that regardless of discharge, there was a preference for positive values, and that this uniquely changed with stage (Fig. 6a). At least 55% of the data always had $C(Z, W^j) > 0$, increasing to 69% at $283.2 \text{ m}^3 \text{ s}^{-1}$, and then slightly declining beyond this flow and stabilizing around 60% (Fig. 6). There were at most 5% of values < -1 , with an average and standard deviation of 3 and 1%, respectively. Contrasting this, values > 1 peaked at 21% at both 283.2 and $597.5 \text{ m}^3 \text{ s}^{-1}$ and declined with increasing discharge. So out of the two extremes, the data exhibited a preference for positive values, with negative values < -1 being very rare. The Mann Whitney U test showed interesting flow dependent aspects of the $C(Z, W^j)$ data sets, where some ranges of flows were significantly different from each other, and others being similar (Table 3). For example, the $8.50 \text{ m}^3 \text{ s}^{-1}$ $C(Z, W^j)$ had p values that were all significant at the 95% level for each other flow, indicating differences in their distributions. For flows between 28.3 – $597.5 \text{ m}^3 \text{ s}^{-1}$, the p values indicated that the series were statistically similar, but not for higher flows. The p values for 1195, 2390, and $3126 \text{ m}^3 \text{ s}^{-1}$ were statistically similar at the 95% level, but not for lower flows.

The quadrant based histogram reveals further insight into the distribution of river geometry with flow (Fig. 6b). The average percentage of $C(Z, W^j)$ for each quadrant across all flows was 31% $\{+W, +Z\}$, 13% $\{+W, -Z\}$, 24% $\{-W, +Z\}$, and 32% $\{-W, -Z\}$, with standard deviations ranging from 2–3%. Percentages of positive $C(Z, W^j)$ was relatively evenly distributed between $\{+W, +Z\}$ and $\{-W, -Z\}$, although the latter was slightly more prevalent. The percent of the data in the $\{+W, +Z\}$ quadrant increased from 26% at $8.50 \text{ m}^3 \text{ s}^{-1}$, peaked at 35% at $598 \text{ m}^3 \text{ s}^{-1}$, decreased to 30%

Analyzing river bed and width oscillations

R. A. Brown and
G. B. Pasternack

Title Page

Abstract

Introduction

Conclusions

References

Tables

Figures

◀

▶

◀

▶

Back

Close

Full Screen / Esc

Printer-friendly Version

Interactive Discussion



Analyzing river bed and width oscillations

R. A. Brown and
G. B. Pasternack

Title Page

Abstract

Introduction

Conclusions

References

Tables

Figures



Back

Close


Full Screen / Esc

Printer-friendly Version

Interactive Discussion



at $1195 \text{ m}^3 \text{ s}^{-1}$ and stabilized for higher flows. Meanwhile, the percent of the data in the $\{-W, -Z\}$ quadrant increased from 29 % at $8.50 \text{ m}^3 \text{ s}^{-1}$ and peaked at 35 %, ~~but~~ at the $283.2 \text{ m}^3 \text{ s}^{-1}$ flow, and then decreased to 30 % at $597.5 \text{ m}^3 \text{ s}^{-1}$. After that it increased to 32 % and stabilized at and beyond $1195 \text{ m}^3 \text{ s}^{-1}$. Both the $\{+W, -Z\}$ and $\{+W, -Z\}$ quadrants followed a similar but opposite trend, reaching a minimum at $283.2 \text{ m}^3 \text{ s}^{-1}$.

Further insights into the positive nature of $C(Z, W^j)$ can be inferred from bivariate Pearson's correlation coefficients of Z and W^j (Fig. 7). Similar to $C(Z, W^j)$ the flow dependent response was that the correlation between Z and W^j increased with flow until $283.2\text{--}597.5 \text{ m}^3 \text{ s}^{-1}$ and then subsequently declined. To further reinforce these results one can also inspect the plot of Z, W^j and $C(Z, W^j)$ for $283.2 \text{ m}^3 \text{ s}^{-1}$, visually showing the synchronous nature of Z and W^j (Fig. 2)  correlations between combinations of W^j show that each series is significantly correlated to the next highest flow, but there is an interesting flow dependent pattern (Fig. 8). Correlations between series decrease with increasing flow, reaching a minimum between 597.5 and $1195 \text{ m}^3 \text{ s}^{-1}$, and then increasing again.

5.3 Are bed and width oscillations quasi-periodic?

The ACF of $C(Z, W^j)$ also showed similar changes with discharge as the above analyses with increases in the presence and magnitude of autocorrelation from 8.50 to $283.2 \text{ m}^3 \text{ s}^{-1}$ and then subsequent decline with increasing flow (Fig. 9a). At the lowest discharge there are approximately 3 broad bands of positive autocorrelation that exceed the white noise threshold, spaced roughly 650 m apart. Only one lag exceeded the AR1 threshold at approximately lag 1400 m . At $28.32 \text{ m}^3 \text{ s}^{-1}$ these three peaks broaden with two peaks exceeding the AR1 threshold, one at 1400 and 2100 m . At the bankfull discharge of $141.6 \text{ m}^3 \text{ s}^{-1}$ the peak at 1500 m diminishes, while the peak at lags $700, 1400$ and 2100 m increase in strength (e.g. correlation magnitude). At $283.2 \text{ m}^3 \text{ s}^{-1}$ there are peaks that exceed both white noise and the AR1 threshold at $700, 1400, 2100$ and 2800 m , with the last one emerging at this discharge. These cor-

relation distances would have a frequency of approximately $0.0014 \text{ cycles m}^{-1}$. Beyond $283.2 \text{ m}^3 \text{ s}^{-1}$ the ACF diminishes rapidly with no peaks that are statistically significant compared to red noise. Overall, the ACF results show that $C(Z, W^j)$ is quasi-periodic from 8.50 to $141.6\text{--}283.2 \text{ m}^3 \text{ s}^{-1}$, but then the periodicity decreases in strength as flow increased.

Similar to ACF analysis, PSD analysis showed quasi-periodic components of $C(Z, W^j)$ exhibiting flow dependence (Fig. 9b). For $8.50\text{--}283.2 \text{ m}^3 \text{ s}^{-1}$ there is a high power band (e.g. $\text{PSD}/\sigma \sim 12$) centered on $0.0014 \text{ cycles m}^{-1}$, which is confirmed from the ACF analysis above. For this range of discharge there are also smaller magnitude peaks of approximately 6 at 0.0007 , 0.002 and $0.0034 \text{ cycles m}^{-1}$, but these are still less than half the magnitude of the 0.0014 band. There's also a high magnitude component at the lowest frequency band that emerges at 28.32 and declines by $283.2 \text{ m}^3 \text{ s}^{-1}$. These low frequency components are commonly associated with first order autoregressive behavior in the data (Shumway and Stoffer, 2010). Beyond $597.5 \text{ m}^3 \text{ s}^{-1}$ the frequency range and magnitude of statistically significant values declines with discharge. Overall, both ACF and PSD results show that $C(Z, W^j)$ is quasi-periodic from 8.50 to $283.2 \text{ m}^3 \text{ s}^{-1}$ but then decreased in strength as flow increased. Further, the PSD results show that the $C(Z, W^j)$ GCS is multiscalar and characterized by a range of statistically significant frequencies.

6 Discussion

6.1 Relating $C(Z, W^j)$ patterns to landforms

The zoomed examples of $C(Z, W^j)$ and the detrended river topography highlight how this type of GCS can be used to characterize the topographic influence on wetted width and bed elevation variability in river corridors. Overall, topographic extremas where Z was either > 1 or < -1 were associated with the largest pools and riffles in the study area, and were characterized by strong peaks (e.g. > 1) in $C(Z, W^j)$. Therefore, the

ESURFD

doi:10.5194/esurf-2015-49

Analyzing river bed and width oscillations

R. A. Brown and
G. B. Pasternack

Title Page

Abstract

Introduction

Conclusions

References

Tables

Figures

⏪

⏩

◀

▶

Back

Close

Full Screen / Esc

Printer-friendly Version

Interactive Discussion



Analyzing river bed and width oscillations

R. A. Brown and
G. B. Pasternack

Title Page

Abstract

Introduction

Conclusions

References

Tables

Figures

◀

▶

◀

▶

Back

Close

Full Screen / Esc

Printer-friendly Version

Interactive Discussion



$C(Z, W^j)$ GCS may be used diagnostically to assess riverine structure and hydraulic function in a continuous manner within a river across an array of flows. While not studied herein, prior work (Brown and Pasternack, 2014) showed that the magnitude of $C(Z, W^j)$ can also be related to flow velocity, though lagged effects do occur. Since the magnitudes can be linked to both unique landforms and flow velocity they may have utility in assessing topographic and hydraulic controls in river corridors.

The examples also provide information on how fluvial landforms such as anabranches, alternate bars, broad riffles, forced pools and point bars can affect $C(Z, W^j)$ with stage (Figs. 4 and 5). Overall, positive peaks in $C(Z, W^j)$ at 8.50 and $283.2 \text{ m}^3 \text{ s}^{-1}$ were associated with the heads of riffles where alluvial bars are widest and centers of constricted pools. Negative peaks in $C(Z, W^j)$ were associated with narrow and high hydraulic controls that presumably function as hydraulic nozzles, and also localized forced pools adjacent to alluvial bars created from flow impinging into the bedrock walls, creating zones of relative low bed elevation and high flow width. The increase in flow from 8.50 to $283.2 \text{ m}^3 \text{ s}^{-1}$ acted to shift the location of these peaks downstream approximately 200 m and broaden their overall shape. In the second example the constricted pools adjacent to the point bar and tailings have positive peaks in $C(Z, W^j)$ that are persistent across all flows. If the tailings were not present on river left in this area the magnitude of $C(Z, W^j)$ would likely decrease as the valley width would be wider. The broad riffle creates a peak in $C(Z, W^j)$ at $8.50 \text{ m}^3 \text{ s}^{-1}$, but this broadens and translates downstream by $283.2 \text{ m}^3 \text{ s}^{-1}$ as the anabranch activates a greater width of flow. The alternate bars channelize flows at $8.50 \text{ m}^3 \text{ s}^{-1}$, but even when flow has already spilled well onto the floodplain at $283.2 \text{ m}^3 \text{ s}^{-1}$ the $C(Z, W^j)$ is still not significantly positive or negative because despite increases in W the Z profile was of relatively low magnitude. This in particular highlights the effect of the standardization process on Z and W , if either one is of low magnitude (e.g. < 1) then it effectively discounts the magnitude of the other, while when the covariate is > 1 it will amplify the other. When flow is contained within the point bars it is relatively constricted, but as flow increased expansions occur near the crossover between bars, causing the rela-

tive width expansion to shift. For flood flows point bars, broad riffles and anabranches all occur in valley expansions, as shown by White et al. (2010).

This study quantitatively supports the idea that river morphology in partially confined valleys is hierarchically nested with broader exogenic as well as channel width scale alluvial controls. In this setting, valley width is constrained across fluvial geomorphic timescales from bedrock, and results show that a top-down organization occurs in the river channel as a result. Each series of W^j was significantly correlated with the next highest flow, but this was lowest between 597.5 and $1195 \text{ m}^3 \text{ s}^{-1}$, where the valley walls begin to be engaged. Since each series of W^j is interdependent on the other (Fig. 8), and bed elevation is highly correlated with width (Fig. 7), this supports the notion that bed elevation adjusts to variations in width and further justifies the positively covarying $C(Z, W^j)$ GCS (Wilkinson et al., 2004; MacWilliams et al., 2006; Caamano et al., 2009; Thompson, 2010; White et al., 2010). White et al. (2010) also show a non-persistent riffle at one of the widest valley expansions. This suggests that when width oscillations reach a certain magnitude inset point bars develop and steer flow at an angle non parallel to the valley centerline. This has the effect of the topographic high point being located not in the widest part of the valley, but phased to the orientation of the lowest lateral bar relief, driven by topographic steering of the bars. For example, at flows below $141.6 \text{ m}^3 \text{ s}^{-1}$ the point bars constrict flow but as flow increases to 283.2 – $597.5 \text{ m}^3 \text{ s}^{-1}$ the bars steer flow transverse to the valley profile, creating expansions at the head or tail of the alternate bars. When the bars are overtopped at $1195 \text{ m}^3 \text{ s}^{-1}$ or greater flow begins to be steered by the valley walls. So this suggests that as large floods deposit valley wide bars in expansions, subsequent more frequent flows erode through these deposits with bed elevation syncing to the self-formed channel width. There's an obvious feedback between the both bed elevation and channel width in this setting, as originally proposed by Richards (1976b) where increased bed elevations presumably deflect flow onto the banks. The exogenous constraint of the bedrock valley walls and large dredger tailings piles also introduce variations in curvature that affect the occurrence of pools, not investigated herein, but this is not consistent throughout.

Analyzing river bed and width oscillations

R. A. Brown and
G. B. Pasternack

[Title Page](#)[Abstract](#)[Introduction](#)[Conclusions](#)[References](#)[Tables](#)[Figures](#)[◀](#)[▶](#)[◀](#)[▶](#)[Back](#)[Close](#)[Full Screen / Esc](#)[Printer-friendly Version](#)[Interactive Discussion](#)

average frequency of 0.0029, 0.0028, and 0.001 cycles m^{-1} . In this study the dominant frequency identified in the PSD analysis was 0.0014 cycles m^{-1} , which is half the MU frequency of both pools and riffles reported by Wyrick and Pasternack (2014). Therefore, it appears that the quasi-periodicity of the $C(Z, W^j)$ GCS is related to the pool-riffle oscillation in the river corridor. This is in agreement with studies based on field investigations and numerical models that relate this observation to quasi-periodic bed and width variations associated with bar-pool topography (Richards, 1976b; Repetto and Tubino, 2001; Carling and Orr, 2002).

The results of this study suggest that self-formed gravel-cobble bedded rivers inset into partially confined valleys organize channel geometry into zones of alternating co-varying bed and width oscillations at discharges with modest recurrence intervals (e.g., 1.2–2.5 years). Rather than select a single type of cross section to maximize energy dissipation to create a uniform cross section geometry at a single channel maintaining flow, commonly referred to as bankfull, it appears that alluvial rivers adjust their channel topography to have cross sections that alternate between those that are wide and shallow and narrow and deep (Huang et al., 2004), with some locations having a prismatic channel form indicative of normative conditions, particularly in transition zones. Presumably, the $C(Z, W^j)$ GCS patterns are also linked to flow dependent patterns of acceleration and deceleration, as the length scales of the GCS were aligned with the spacing of erosional and depositional landforms such as bars and pools. This aspect is supported by two studies on the LYR. First, Sawyer et al. (2010) showed that stage dependent flow convergence maintained bed relief by topographically mediated changes in peak velocity and shear stress. Additionally, Strom and Pasternack (2016) showed that peak zones of velocity undergo variable changes in their location with discharge. In this case the zones of peak velocity patches underwent complex changes from being associated with narrow topographic high points at base flows $\{-W^j, +Z\}$ to topographic low points where flow width is constricted at high flows $\{-W^j, -Z\}$. Further, this study is aligned with prior work that suggests a single frequency or flow does not fully describe

Analyzing river bed and width oscillations

R. A. Brown and
G. B. Pasternack

Title Page

Abstract

Introduction

Conclusions

References

Tables

Figures



Back

Close

Full Screen / Esc

Printer-friendly Version

Interactive Discussion



the relationship between $C\{Z, W^j\}$, and presumably channel morphology (Wyrick and Pasternack, 2014) but that a continuum of frequencies are present (Chin, 2002).

6.3 Broader implications

This study quantified relationships between width and bed elevation in a partly confined and incising gravel-cobble bedded river, as well as for the first time how they change with stage. The results of this study are relevant to river restoration and flow reregulation in that a wide array of discharges beyond a single channel forming flow are needed for alluvial channel maintenance (Parker et al., 2003). This is supported by the results that show gradual changes in channel organization within a band of discharges with recurrence intervals ranging from 1.2–2.5 years, and two fold range in absolute discharges. Further, while the length scales of covarying bed and width undulations are approximate to the spacing of bars and pools in the study area, they are quite complex and lack explicit cutoffs that illustrate power in a singular frequency band. Thus, river restoration efforts that specify modal values of bedforms may overly simplify the physical structure of rivers with unknown consequences to ecological communities and key functions that are the focus of such efforts. Designs need to mimic the multiscale nature of self-formed topography by incorporating GCS into river engineering (Brown et al., 2015) or somehow insure that simpler uniscale designs will actually evolve into multiscale ones given available flows and anthropogenic boundary constraints.

This study has potential implications for analyzing the effect of flow dependent responses to topography and physical habitat in river corridors. Valley and channel widths have shown to be very predictive in predicting the intrinsic potential of salmon habitat (Burnett et al., 2007). Further, the role of covarying bed and width undulations in modulating velocity signals and topographic change has implications to the maintenance of geomorphic domains used by aquatic organisms. As one example, consider that adult salmonids use positively covarying zones such as riffles (e.g. $+W^j, +Z$) for spawning and pools (e.g. $-W^j, -Z$) for holding (Bjorn and Reiser, 1991). In the study

Analyzing river bed and width oscillations

R. A. Brown and
G. B. Pasternack

Title Page	
Abstract	Introduction
Conclusions	References
Tables	Figures
◀	▶
◀	▶
Back	Close
Full Screen / Esc	
Printer-friendly Version	
Interactive Discussion	



Analyzing river bed and width oscillations

R. A. Brown and
G. B. Pasternack

Title Page

Abstract

Introduction

Conclusions

References

Tables

Figures



Back

Close

Full Screen / Esc

Printer-friendly Version

Interactive Discussion



reach Pasternack et al. (2014) showed that 77% of spawning occurred in riffles and chute morphologic units, which are at or adjacent to areas where $C(Z, W^j) > 0$ (Figs. 4 and 5), supporting this idea. The presence and structure of covarying bed and width undulations is also thought to be important indirectly for juvenile salmonids that require shallow and low velocity zones for refugia during large floods. For example the expansions that occur at the head of riffles would presumably provide shallow depths and moderate velocities needed for flood refugia. In the absence of positive bed relief, and zones of $+W$, $+Z$, flow refugia zones would be hydrologically disconnected from overbank areas, impacting the ability of juvenile salmon to utilize these areas as refugia during floods and potentially leading to population level declines (Nickelson et al., 1992). Future work should better constrain the utility of GCS concepts in assessing aquatic habitat.

Lastly, it's possible that the $C(Z, W^j)$ GCS could be used across rivers as a comparative proxy in remote sensing applications to determine how the topographic structure of rivers change with flow. LiDAR and analytical methods for developing bed topography in rivers has improved considerably (McKean et al., 2009). For example, Gessese et al. (2011) derived an analytical expression for determining bed topography from water surface elevations, which can be obtained from LiDAR (Magirl et al., 2005). Assuming one has an adequate topographic data set, whether numerical flow modeling is needed to generate wetted width data sets places a considerable constraint on performing this type of analysis. This could potentially be relaxed, especially at flows above bankfull, using a constant water slope approximation for various flow stages. At smaller discharges in rivers there are typically defects in the water surface elevation, where the bed topography exerts a strong control (e.g. Brown and Pasternack, 2008). However, many studies suggest that on large alluvial rivers bankfull and flood profiles show that they generally flatten and smoothen once bed forms and large roughness elements such as gravel bars are effectively submerged. In this case, one can then detrend the river corridor and take serial width measurements associated at various heights above the riverbed (Gangodagamage et al., 2007). The height above the river then

References

- Abu-Aly, T. R., Pasternack, G. B., Wyrick, J. R., Barker, R., Massa, D., and Johnson, T.: Effects of LiDAR-derived, spatially distributed vegetation roughness on two-dimensional hydraulics in a gravel-cobble river at flows of 0.2 to 20 times bankfull, *Geomorphology*, 206, 468–482, doi:10.1016/j.geomorph.2013.10.017, 2014.
- Adler, L. L.: Adjustment of Yuba River, California, to the influx of hydraulic mining debris, 1849–1979, M. A. thesis, Geography Department, University of California, Los Angeles, 1980.
- Andrews, E. D.: Effective and bankfull discharges of streams in the Yampa River basin, Colorado and Wyoming, *J. Hydrol.*, 46, 311–330, 1980.
- Bejan, A. and Lorente, S.: The constructal law of design and evolution in nature, *Philos. T. Roy. Soc. B*, 365, 1335–1347, doi:10.1098/rstb.2009.0302, 2010.
- Bjorn, T. C. and Reiser, D. W.: Habitat requirements of salmonids in streams, in: *Influences of Forest and Rangeland Management on Salmonid Fishes and Their Habitats*, edited by Meehan, W. R., Special Publication 19, American Fisheries Society, Bethesda, MD, 83–138, 1991.
- Brown, R. A.: *The Analysis and Synthesis of River Topography*, PhD thesis, University Of California, Davis, 187 pp., 2014.
- Brown, R. A. and Pasternack, G. B.: Engineered channel controls limiting spawning habitat rehabilitation success on regulated gravel-bed rivers, *Geomorphology*, 97, 631–654, 2008.
- Brown, R. A. and Pasternack, G. B.: Hydrologic and topographic variability modulate channel change in mountain rivers, *J. Hydrol.*, 510, 551–564, doi:10.1016/j.jhydrol.2013.12.048, 2014.
- Brown, R. A., Pasternack, G. B., and Lin, T.: The topographic design of river channels for form-process linkages, *Environ. Manage.*, doi:10.1007/s00267-015-0648-0, 2015.
- Burnett, K. M., Reeves, G. H., Miller, D. J., Clarke, S., Vance-Borland, K., and Christiansen, K.: Distribution of salmon-habitat potential relative to landscape characteristics and implications for conservation, *Ecol. Appl.*, 17, 66–80, doi:10.1890/1051-0761(2007)017[0066:DOSPRT]2.0.CO;2, 2007.
- Caamaño, D., Goodwin, P., and Buffington, J. M.: Unifying criterion for the velocity reversal hypothesis in gravel-bed rivers, *J. Hydraul. Eng.*, 135, 66–70, 2009.
- Carboneau, P., Fonstad, M. A., Marcus, W. A., and Dugdale, S. J.: Making riverscapes real, *Geomorphology*, 137, 74–86, doi:10.1016/j.geomorph.2010.09.030, 2012.

Analyzing river bed and width oscillations

R. A. Brown and
G. B. Pasternack

Title Page

Abstract

Introduction

Conclusions

References

Tables

Figures



Back

Close

Full Screen / Esc

Printer-friendly Version

Interactive Discussion



Analyzing river bed and width oscillations

R. A. Brown and
G. B. Pasternack

Title Page

Abstract

Introduction

Conclusions

References

Tables

Figures

◀

▶

◀

▶

Back

Close

Full Screen / Esc

Printer-friendly Version

Interactive Discussion



- Carley, J. K., Pasternack, G. B., Wyrick, J. R., Barker, J. R., Bratovich, P. M., Massa, D., Reedy, G., and Johnson, T. R.: Significant decadal channel change 58–67 years post-dam accounting for uncertainty in topographic change detection between contour maps and point cloud models, *Geomorphology*, 179, 71–88, doi:10.1016/j.geomorph.2012.08.001, 2012.
- 5 Carling, P. A. and Orr, H. G.: Morphology of riffle-pool sequences in the River Severn, England, *Earth Surf. Proc. Land.*, 2, 369–384, doi:10.1002/(SICI)1096-9837(200004)25:4<369::AID-ESP60>3.0.CO;2-M, 2000.
- Carter, G., Knapp, C., and Nuttall, A.: Estimation of the magnitude-squared coherence function via overlapped fast Fourier transform processing, *IEEE T. Acoust. Speech*, 21, 337–344, doi:10.1109/TAU.1973.1162496, 1973.
- 10 Cherkauer, D. S.: Minimization of power expenditure in a riffle-pool alluvial channel, *Water Resour. Res.*, 9, 1613–1628, 1973.
- Chin, A.: The periodic nature of step-pool streams, *Am. J. Sci.*, 302, 144–167, 2002.
- Church, M.: Multiple scales in rivers, in: *Developments in Earth Surface Processes*, vol. 11, edited by: Habersack, H., Piégay, H., and Rinaldi, M., Elsevier, pp. 3–28, ISSN 0928-2025, ISBN 9780444528612, doi:10.1016/S0928-2025(07)11111-1, 2006.
- 15 Colombini, M., Seminara, G., and Tubino, M.: Finite-amplitude alternate bars, *J. Fluid Mech.*, 181, 213–232, doi:10.1017/S0022112087002064, 1987.
- Cox, N. J.: On the estimation of spatial autocorrelation in geomorphology, *Earth Surf. Proc. Land.*, 8, 89–93, doi:10.1002/esp.3290080109, 1983.
- 20 DeAlmeida, G. A. M. and Rodriguez, J. F.: Spontaneous formation and degradation of pool-riffle morphology and sediment sorting using a simple fractional transport model, *Geophys. Res. Lett.*, 39, L06407, doi:10.1029/2012GL051059, 2012.
- Dolan, R., Howard, A., and Trimble, D.: Structural control of the rapids and pools of the Colorado River in the Grand Canyon, *Science*, 10, 629–631, doi:10.1126/science.202.4368.629, 1978.
- 25 Gangodagamage, C., Barnes, E., and Fofoula Georgiou, E.: Scaling in river corridor widths depicts organization in valley morphology, *Geomorphology*, 91, 198–215, doi:10.1016/j.geomorph.2007.04.014, 2007.
- 30 Gessese, A. F., Sellier, M., Van Houten, E., and Smart, G.: Reconstruction of river bed topography from free surface data using a direct numerical approach in one-dimensional shallow water flow, *Inverse Probl.*, 27, 1–12, doi:10.1088/0266-5611/27/2/025001, 2011.

- Harrison, L. R. and Keller, E. A.: Modeling forced pool–riffle hydraulics in a boulder-bed stream, southern California, *Geomorphology*, 83, 232–248, doi:10.1016/j.geomorph.2006.02.024, 2007.
- Hernandez, G.: Time series, periodograms, and significance, *J. Geophys. Res.*, 104, 10355–10368, doi:10.1029/1999JA900026, 1999.
- Hey, R. D. and Thorne, C. R.: Stable channels with mobile gravel beds, *J. Hydraul. Eng.*, 112, 671–689, 1986.
- Huang, H. Q., Chang, H. H., and Nanson, G. C.: Minimum energy as the general form of critical flow and maximum flow efficiency and for explaining variations in river channel pattern, *Water Resour. Res.*, 40, W04502, doi:10.1029/2003WR002539, 2004.
- Jackson, J. R., Pasternack, G. B., and Wyrick, J. R.: Substrate of the Lower Yuba River, prepared for the Yuba Accord River Management Team, University of California, Davis, CA, 61 pp., 2013.
- James, L. A., Singer, M. B., and Ghoshal, S.: Historical channel changes in the lower Yuba and Feather Rivers, California: long-term effects of contrasting river-management strategies, *Geol. S. Am. S.*, 451, 57–81, doi:10.1130/2009.2451(04), 2009.
- Keller, E.: Areal sorting of bed-load material: the hypothesis of velocity reversal, *Geol. Soc. Am. Bull.*, 82, 753–756, 1971.
- Keller, E. A. and Melhorn, W. N.: Rhythmic spacing and origin of pools and riffles, *Geol. Soc. Am. Bull.*, 89, 723–730, doi:10.1130/0016-7606(1978)89<723:RSAOOP>2.0.CO;2, 1978.
- Knighton, A.: Models of stream bed topography at the reach scale, *J. Hydrol.*, 60, 105–121, doi:10.1016/0022-1694(83)90016-1, 1983.
- Leopold, L. B. and Langbein, W. B.: *The Concept of Entropy in Landscape Evolution*, US Geological Survey Professional Paper 500-A, US government, Washington, DC, USA, 20 pp., 1962.
- MacWilliams Jr., M. L., Wheaton, J. M., Pasternack, G. B., Street, R. L., and Kitanidis, P. K.: Flow convergence routing hypothesis for pool–riffle maintenance in alluvial rivers, *Water Resour. Res.*, 42, W10427, doi:10.1029/2005WR004391, 2006.
- Madej, M. A.: Development of channel organization and roughness following sediment pulses in single-thread, gravel bed rivers, *Water Resour. Res.*, 37, 2259–2272, doi:10.1029/2001WR000229, 2001.

ESURFD

doi:10.5194/esurf-2015-49

Analyzing river bed and width oscillations

R. A. Brown and
G. B. Pasternack

[Title Page](#)[Abstract](#)[Introduction](#)[Conclusions](#)[References](#)[Tables](#)[Figures](#)[Back](#)[Close](#)[Full Screen / Esc](#)[Printer-friendly Version](#)[Interactive Discussion](#)

Analyzing river bed and width oscillations

R. A. Brown and
G. B. Pasternack

Title Page

Abstract

Introduction

Conclusions

References

Tables

Figures

◀

▶

◀

▶

Back

Close

Full Screen / Esc

Printer-friendly Version

Interactive Discussion



Magirl, C. S., Webb, R. H., and Griffiths, P. G.: Changes in the water surface profile of the Colorado River in Grand Canyon, Arizona, between 1923 and 2000, *Water Resour. Res.*, 41, W05021, doi:10.1029/2003WR002519, 2005.

5 McKean, J. A., Isaac, D. J., and Wright, C. W.: Geomorphic controls on salmon nesting patterns described by a new, narrow-beam terrestrial–aquatic lidar, *Front. Ecol. Environ.*, 6, 125–130, doi:10.1890/070109, 2008.

McKean, J., Nagel, D., Tonina, D., Bailey, P., Wright, C. W., Bohn, C., and Nayegandhi, A.: Remote sensing of channels and riparian zones with a narrow-beam aquatic-terrestrial lidar, *Remote Sensing*, 1, 1065–1096, doi:10.3390/rs1041065, 2009.

10 Melton, M. A.: Methods for measuring the effect of environmental factors on channel properties, *J. Geophys. Res.*, 67, 1485–1490, doi:10.1029/JZ067i004p01485, 1962.

Milan, D. J., Heritage, G. L., Large, A. R.G, and Charlton, M. E.: Stage dependent variability in tractive force distribution through a riffle-pool sequence, *Catena*, 44, 85–109, 2001.

Milne, J. A.: Bed-material size and the riffle-pool sequence, *Sedimentology*, 29, 267–278, doi:10.1111/j.1365-3091.1982.tb01723.x, 1982.

15 Nickelson, T. A., Rodgers, J., Johnson, S. L., and Solazzi, M. F.: Seasonal changes in habitat use by juvenile Coho Salmon (*Oncorhynchus kisutch*) in Oregon coastal streams, *Can. J. Fish. Aquat. Sci.*, 49, 783–789, doi:10.1139/f92-088, 1992.

Nolan, K. M., Lisle, T. E., and Kelsey, H. M.: Bankfull discharge and sediment transport in north-western California, in: *Erosion and Sedimentation in the Pacific Rim (Proceedings of the Corvallis Symposium, August 1987)*, edited by: Beschta, R., Blinn, T., Grant, G. E., Swanson, F. J., and Ice, G. G., International Association of Hydrological Sciences Pub. No. 165, Corvallis, Oregon, 439–449, 1987.

20 Parker, G., Toro-Escobar, C. M., Ramey, M., and Beck, S.: The effect of floodwater extraction on the morphology of mountain streams, *J. Hydraul. Eng.*, 129, 885–895, 2003.

Pasternack, G. B., Tu, D., and Wyrick, J. R.: Chinook adult spawning physical habitat of the lower Yuba River, prepared for the Yuba Accord River Management Team, University of California, Davis, CA, 154 pp., 2014.

25 Pike, R. J., Evans, I., and Hengl, T.: *Geomorphometry: a brief guide*, In: *Geomorphometry – Concepts, Software, Applications, Series Developments in Soil Sciences*, vol. 33, edited by: Hengl, T., and Reuter, H. I., Elsevier, 3–33, ISBN 978-0-12-374345-9, 2008.

Analyzing river bed and width oscillations

R. A. Brown and
G. B. Pasternack

Title Page

Abstract

Introduction

Conclusions

References

Tables

Figures



Back

Close

Full Screen / Esc

Printer-friendly Version

Interactive Discussion



Rayburg, S. C. and Neave, M.: Assessing morphologic complexity and diversity in river systems using three-dimensional asymmetry indices for bed elements, bedforms and bar units, *River Res. Appl.*, 24, 1343–1361, doi:10.1002/rra.1096, 2008.

Rendell, H. and Alexander, D.: Note on some spatial and temporal variations in ephemeral channel form, *Geol. Soc. Am. Bull.*, 9, 761–772, doi:10.1130/0016-7606(1979)90<761:NOSSAT>2.0.CO;2, 1979.

Repetto, R. and Tubino, M.: Topographic expressions of bars in channels with variable width, *Phys. Chem. Earth Pt. B*, 26, 71–76, 2001.

Richards, K. S.: The morphology of riffle-pool sequences, *Earth Surf. Processes*, 1, 71–88, doi:10.1002/esp.3290010108, 1976a.

Richards, K. S.: Channel width and the riffle-pool sequence, *Geol. Soc. Am. Bull.*, 87, 883–890, 1976b.

Richards, K. S.: *Stochastic Processes in one Dimension: an Introduction. Concepts and Techniques in Modern Geography No. 23*, London, UK, 30 pp., 1979.

Richter, B. D., Braun, D. P., Mendelson, M. A., and Master, L. L.: Threats to imperiled freshwater fauna, *Conserv. Biol.*, 11, 1081–1093, 1997.

Salas, J. D.: *Applied Modeling of Hydrologic Time Series*, Water Resources Publications, Littleton, CO, 1980.

Sawyer, A. M., Pasternack, G. B., Moir, H. J., and Fulton, A. A.: Riffle-pool maintenance and flow convergence routing confirmed on a large gravel bed river, *Geomorphology*, 114, 143–160, 2010.

Shumway, R. H. and Stoffer, D. S.: *Time Series Analysis and Its Applications: With R Examples*, Springer US, New York, NY, USA, 505 pp., 2010.

Strom, M. and Pasternack, G. B.: Reenvisioning velocity reversal as a diversity of hydraulic patch behaviors, *Hydrol. Process.*, accepted, 2016.

Thompson, D. M.: The velocity-reversal hypothesis revisited, *Prog. Phys. Geog.*, 35, 123–132, doi:10.1177/0309133310369921, 2010.

Trauth, M. H., Gebbers, R., Marwan, N., and Sillmann, E.: *MATLAB Recipes for Earth Sciences*, Springer, Berlin, Germany, 2006.

White, J. Q., Pasternack, G. B., and Moir, H. J.: Valley width variation influences riffle–pool location and persistence on a rapidly incising gravel-bed river, *Geomorphology*, 121, 206–221, doi:10.1016/j.geomorph.2010.04.012, 2010.

Analyzing river bed and width oscillations

R. A. Brown and
G. B. Pasternack

Title Page

Abstract

Introduction

Conclusions

References

Tables

Figures

⏪

⏩

◀

▶

Back

Close

Full Screen / Esc

Printer-friendly Version

Interactive Discussion



Wilkinson, S. N., Keller, R. J., and Rutherford, I. D.: Phase-shifts in shear stress as an explanation for the maintenance of pool–riffle sequences, *Earth Surf. Proc. Land.*, 29, 737–753, doi:10.1002/esp.1066, 2004.

Williams, G. P.: Bank-full discharge of rivers, *Water Resour. Res.*, 14, 1141–1154, doi:10.1029/WR014i006p01141, 1978.

Wohl, E. E., Thompson, D. M., and Miller, A. J.: Canyons with undulating walls, *Geol. Soc. Am. Bull.*, 111, 949–959, 1999.

Wyrick, J. R. and Pasternack, G. B.: Geospatial organization of fluvial landforms in a gravel–cobble river: beyond the riffle–pool couplet, *Geomorphology*, 213, 48–65, doi:10.1016/j.geomorph.2013.12.040, 2014.

Wyrick, J. R. and Pasternack, G. B.: Landforms of the Lower Yuba River, University of California, Davis, 2012.

Yalin, M. S.: *Mechanics of Sediment Transport*, Elsevier, Oxford, UK, 1977.

Yang, C. T.: Potential energy and stream morphology, *Water Resour. Res.*, 7, 1567–1574, doi:10.1029/WR007i002p00311, 1971.

Analyzing river bed and width oscillations

R. A. Brown and
G. B. Pasternack

Title Page

Abstract

Introduction

Conclusions

References

Tables

Figures



Back

Close

Full Screen / Esc

Printer-friendly Version

Interactive Discussion



Table 1. Flows analyzed and their approximate annual recurrence intervals.

Q ($\text{m}^3 \text{s}^{-1}$)	Approximate Recurrence Interval
8.50	1
28.32	1.03
141.6	1.2
283.2	1.5
597.5	2.5
1195	4.7
2390	12.7
3126	20

Analyzing river bed and width oscillations

R. A. Brown and
G. B. Pasternack

Table 2. Linear trend models and R^2 for Z and W^j used in detrending each series.

Discharge ($\text{m}^3 \text{s}^{-1}$)	Top width		Bed elevation	
	Linear trend model	R^2	Linear trend model	R^2
8.50	$y = -0.0016x + 193.03$	0.0231	$y = 0.002x + 194.2$	0.8727
28.32	$y = -0.0025x + 234.27$	0.0429	$y = 0.002x + 194.26$	0.8713
141.6	$y = -0.003x + 301.61$	0.0423	$y = 0.0021x + 194.04$	0.8731
283.2	$y = -0.0002x + 332.87$	0.0002	$y = 0.0021x + 194.23$	0.8710
597.5	$y = -0.0101x + 528.6$	0.2286	$y = 0.0021x + 194.16$	0.8711
1195	$y = -0.0133x + 665.02$	0.3037	$y = 0.0021x + 194.29$	0.8703
2390	$y = -0.012x + 710.57$	0.2420	$y = 0.0022x + 193.92$	0.8736
3126	$y = -0.0121x + 733.12$	0.2437	$y = 0.0022x + 193.94$	0.8733

Title Page

Abstract

Introduction

Conclusions

References

Tables

Figures

◀

▶

◀

▶

Back

Close

Full Screen / Esc

Printer-friendly Version

Interactive Discussion



Analyzing river bed and width oscillations

R. A. Brown and
G. B. Pasternack

Table 3. Mann–Whitney U test p values amongst all combinations of Z and W^j at the 95 % level.

	8.50	28.32	141.6	283.2	597.5	1195	2390	3126
8.50		0.0002	0.0000	0.0000	0.0000	0.0046	0.0239	0.0130
28.32			0.0889	0.0009	0.0716	0.2735	0.1219	0.1805
141.6				0.0655	0.9973	0.0032	0.0009	0.0019
283.2					0.1031	0.0000	0.0000	0.0000
597.5						0.0032	0.0005	0.0010
1195							0.6967	0.8885
2390								0.8176
3126								

Title Page

Abstract

Introduction

Conclusions

References

Tables

Figures



Back

Close

Full Screen / Esc

Printer-friendly Version

Interactive Discussion



Analyzing river bed and width oscillations

R. A. Brown and
G. B. Pasternack

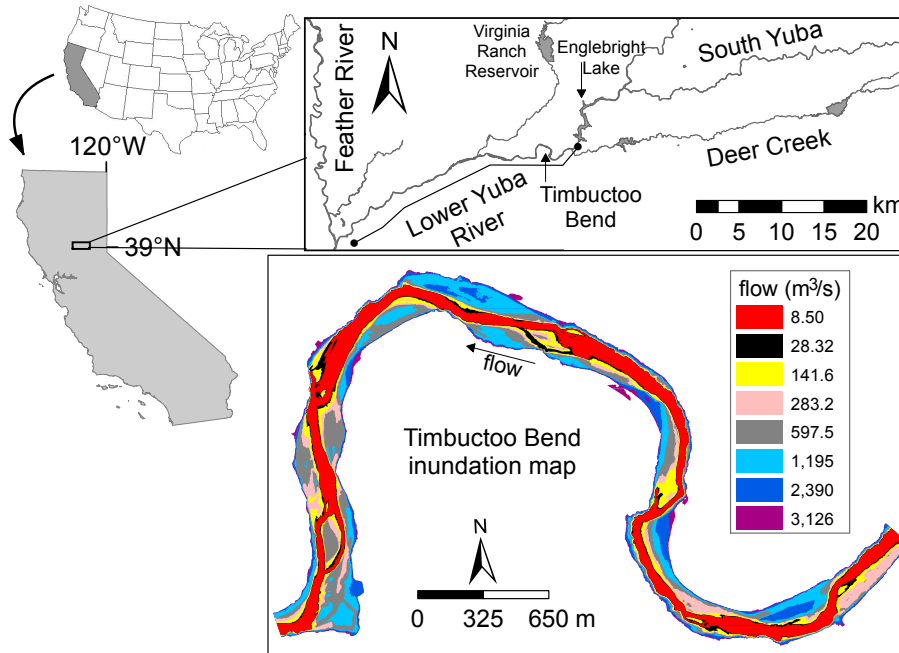


Figure 1. Regional and vicinity map of the lower Yuba River and extent of study segment showing inundation extents predicted by the 2-D model.

Title Page	
Abstract	Introduction
Conclusions	References
Tables	Figures
◀	▶
◀	▶
Back	Close
Full Screen / Esc	
Printer-friendly Version	
Interactive Discussion	



Analyzing river bed and width oscillations

R. A. Brown and
G. B. Pasternack

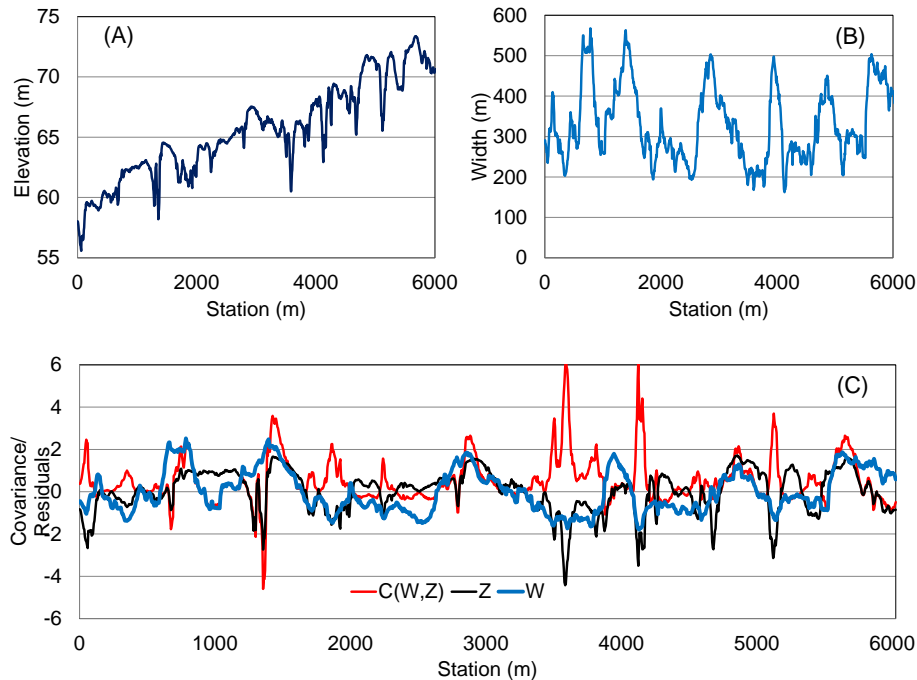


Figure 2. Raw bed profile **(a)** and flow width **(b)** series for $283.2 \text{ m}^3 \text{ s}^{-1}$. After detrending and standardizing both series values of Z (black line in **c**) and W (blue line in **c**) are multiplied by each other generating the $C(Z, W^j)$ GCS (red line in **c**).

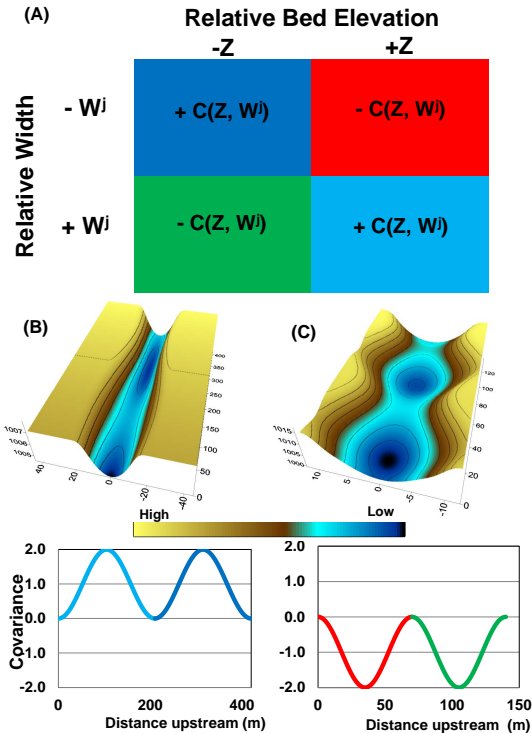


Figure 3. Conceptual key for interpreting $C(Z, W^j)$ geomorphic covariance structures **(a)**. For quadrant 1 Z and W^j are both relatively high, so that implies wide and shallow areas associated with deposition. Conversely, in quadrant 2 Z is relatively low, but W^j is relatively high, which implies deep and wide cross areas, which implies that these areas may have been scoured at larger flows. In quadrant 3 Z and W^j are both relatively low, so that implies narrow and deep areas associated with erosion. Finally, in quadrant 4 Z is relatively high and W^j is relatively low, so that implies narrow and topographically high areas. Prototypical channels and GCS with positive **(b)**, and negative **(c)** $C(Z, W^j)$ colored according to **(a)**.

Analyzing river bed and width oscillations

R. A. Brown and
G. B. Pasternack

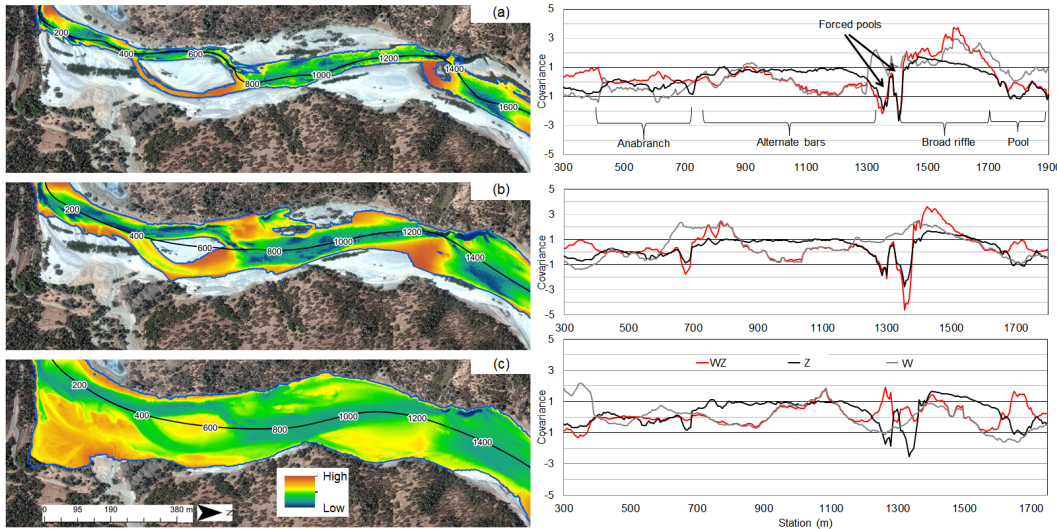


Figure 4. Example section of detrended bed topography and plots of Z , W , and $C(Z, W^j)$ for $8.50 \text{ m}^3 \text{ s}^{-1}$ (a), $283.2 \text{ m}^3 \text{ s}^{-1}$ (b), $3126 \text{ m}^3 \text{ s}^{-1}$ (c) in the middle of the study area. The detrended topography has been clipped to the wetted extents for each flow to accentuate relative bed features. Flow dependent sample pathways are shown for stationing reference between the image and the plots.

Title Page

Abstract Introduction

Conclusions References

Tables Figures

◀ ▶

◀ ▶

Back Close

Full Screen / Esc

Printer-friendly Version

Interactive Discussion



Analyzing river bed and width oscillations

R. A. Brown and
G. B. Pasternack

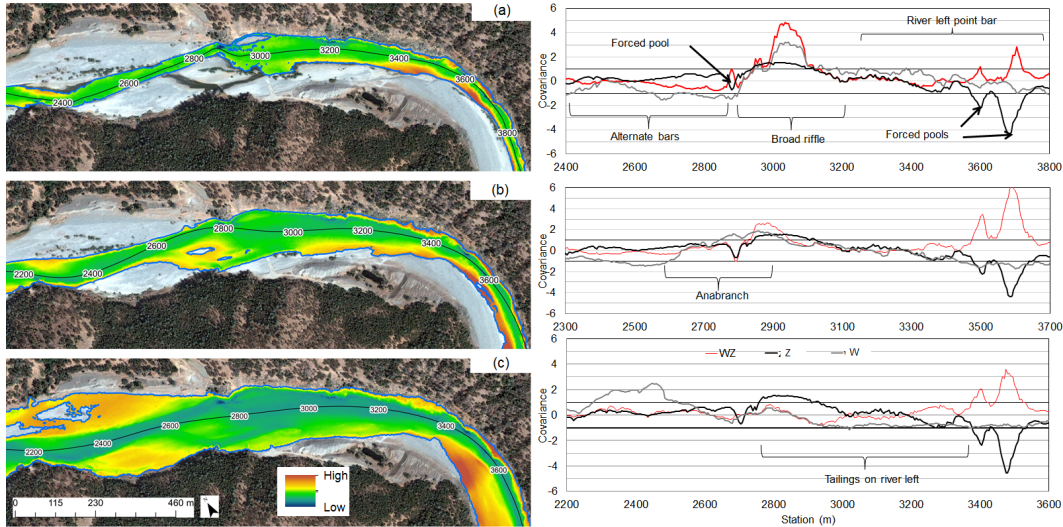


Figure 5. Example section of detrended bed topography and plots of Z , W , and $C(Z, W^j)$ for $8.50 \text{ m}^3 \text{ s}^{-1}$ (a), $283.2 \text{ m}^3 \text{ s}^{-1}$ (b), $3126 \text{ m}^3 \text{ s}^{-1}$ (c) at the lower extent of the study area. The detrended topography has been clipped to the wetted extents for each flow to accentuate relative bed features. Flow dependent sample pathways are shown for stationing reference between the image and the plots.

Title Page

Abstract Introduction

Conclusions References

Tables Figures

◀ ▶

◀ ▶

Back Close

Full Screen / Esc

Printer-friendly Version

Interactive Discussion



Analyzing river bed and width oscillations

R. A. Brown and
G. B. Pasternack

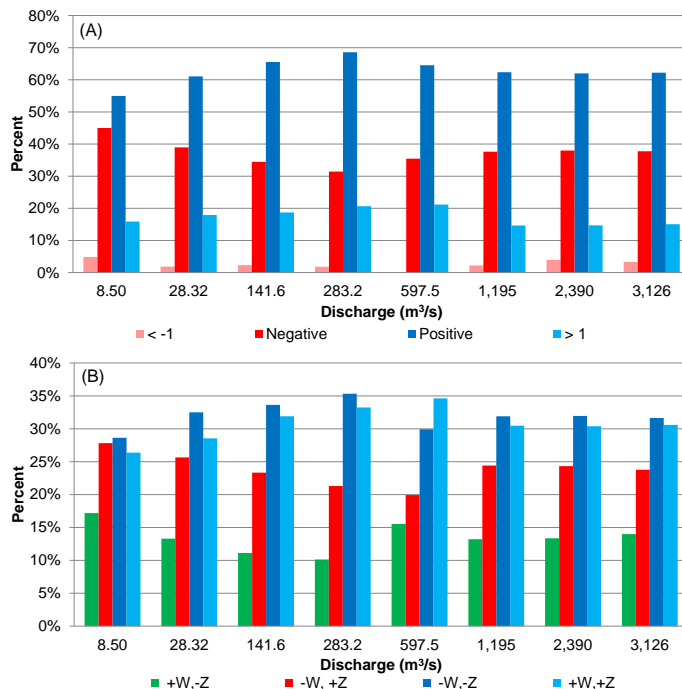


Figure 6. Histogram of $C(Z, W^j)$ classified by positive and negative values as well as $>$ and $<$ 1 (a). Also shown is a histogram classified by quadrant (b). Both illustrate an overall preference for $C(Z, W^j) > 0$ with increasing discharge and also illustrating an increasing preference for positive values of $C(Z, W^j) > 1$ up until $283.2 \text{ m}^3 \text{ s}^{-1}$ after which it declines. Colors represent bin centered values.

Analyzing river bed and width oscillations

R. A. Brown and
G. B. Pasternack

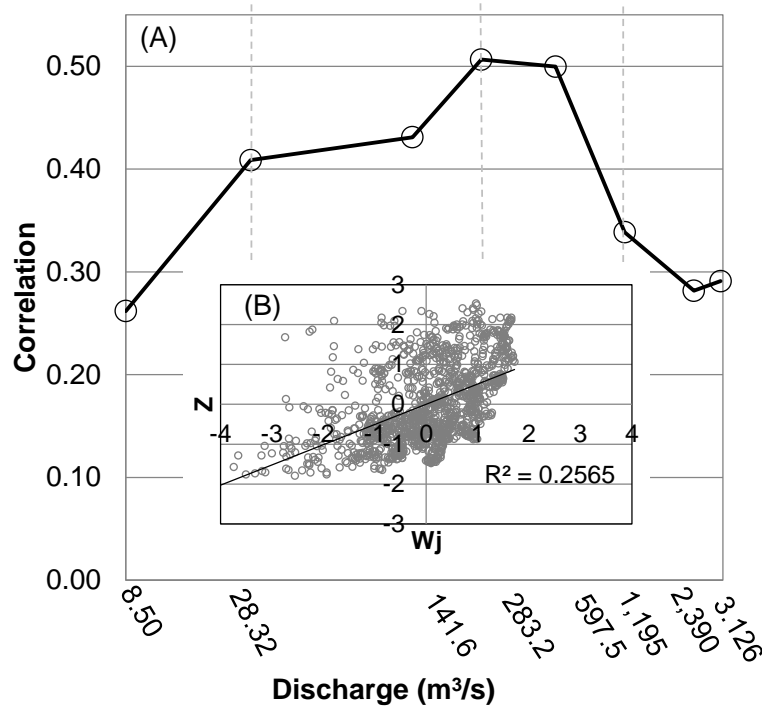


Figure 7. Pearson's correlation coefficient for Z and W^j (a) between each flow and an example scatter plot of Z vs. W^j at $283.2 \text{ m}^3 \text{ s}^{-1}$ (b).

Title Page

Abstract Introduction

Conclusions References

Tables Figures

◀ ▶

◀ ▶

Back Close

Full Screen / Esc

Printer-friendly Version

Interactive Discussion



ESURFD

doi:10.5194/esurf-2015-49

Analyzing river bed and width oscillations

R. A. Brown and
G. B. Pasternack

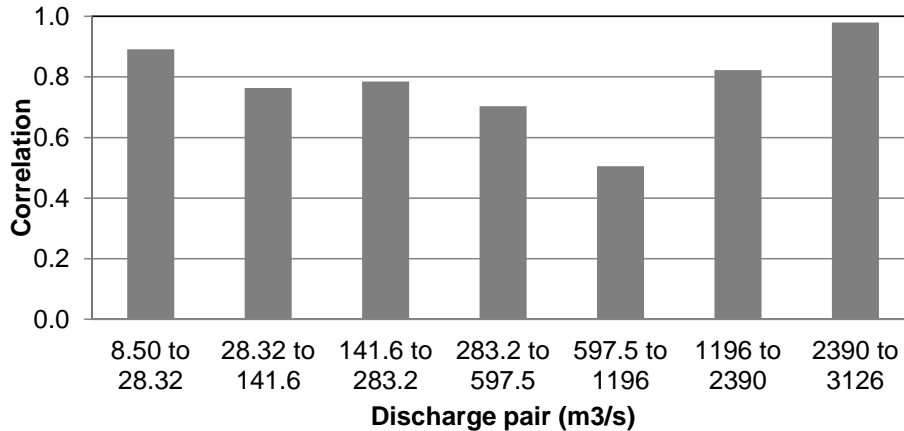


Figure 8. Pearson's correlation coefficient for sequential pairs of flow dependent wetted width series.

Title Page

Abstract Introduction

Conclusions References

Tables Figures

◀ ▶

◀ ▶

Back Close

Full Screen / Esc

Printer-friendly Version

Interactive Discussion



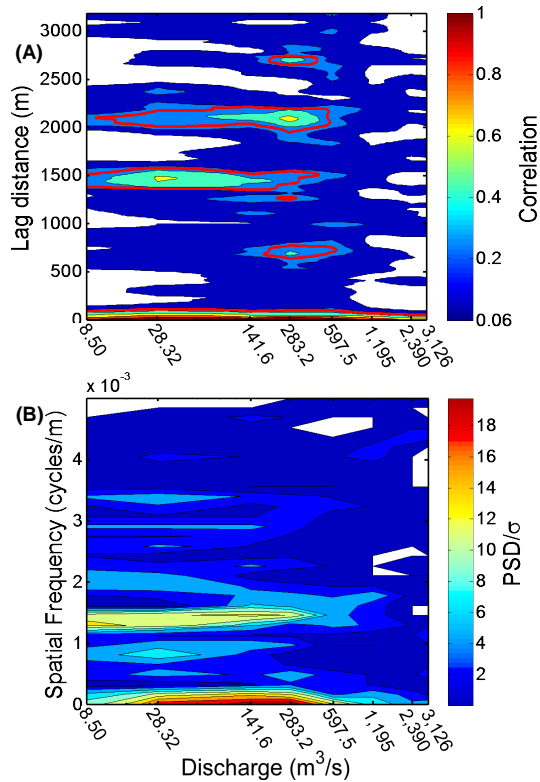


Figure 9. Autocorrelation **(a)** and PSD **(b)** of $C(Z, W^j)$ with increasing flow. For the ACF plot **(a)**, only values exceeding white noise at the 95 % level are shown and the red contour demarcates the 95 % level for an AR1 process (red noise). For the PSD plot **(b)** only values exceeding white noise at the 95 % level are shown.

Analyzing river bed and width oscillations

R. A. Brown and
G. B. Pasternack

Title Page

Abstract Introduction

Conclusions References

Tables Figures

◀ ▶

◀ ▶

Back Close

Full Screen / Esc

Printer-friendly Version

Interactive Discussion

